Journal of Engineering Science and Technology
Special Issue on Development of Sustainability Systems - I, 240 - 254

FATIGUE AND HARDNESS BEHAVIOR OF AL-2CU-2MG ALLOY DUE TO TITANIUM DIOXIDE AND SILICON CARBIDE NANOADDITIVES

SALMAN H. OMRAN[1], ABDULLAH D. ASSI[2], MOAZ H. ALI.[3], AHMED A. SHANDOOK[4,*], LUAY H. ABBUD[5], HASANAIN A. ABDUL WAHHAB[6]

[1]Energy and Renewable Energies Technology Center, University of Technology- Iraq
[2]Mechanical Engineering Department, College of Engineering, University of Baghdad, Iraq
[3]Department of Computer Engineering Techniques, Al-Safwa University College, Karbala, Iraq,
[4]Mechanical Engineering Department, University of Technology, Iraq
[5]Air conditioning and Refrigeration Techniques Engineering Department, Al-Mustaqbal University College, Babil, Iraq
[6]Training and Workshop Center, University of Technology, Iraq
*Corresponding Author: Ahmed.A.Shandookh@uotechnology.edi.iq

Abstract

The current research deals with preparing rods of 10 cm in length and 2 cm in diameter from aluminium matrix composites (AMC) with a metal base represented by (Al-2Cu-2Mg) alloy supported by titanium oxide (TiO_2) nanoparticles on the one hand and silicon carbide (SiC) nanoparticles on the other with different weight ratios (0,3,6 and 9 wt.%). The base alloy and composite materials were prepared by stir casting technique (SCT) using the vortex technique to disperse the stiffeners in the base alloy floor. Two main groups of composites were prepared. The first group was a nanoparticle titanium dioxide (TiO_2) reinforced composite material, while the second group included a fine-reinforced composite material silicon carbide (SiC) nanoparticle. The study included the effect of solution heat treatment at 500 °C and the subsequent formation process. The results showed an increase in fatigue strength and hardness values with increased percentages of added stiffening nanoparticles. As for the effect of the quality of the added hardening granules on the mechanical properties, it was observed that there was a noticeable increase in the fatigue strength and hardness values of the composite material reinforced with TiO_2 nanoparticles compared to SiC nanoparticles, which acquired a higher value than that of the base alloy.

Keywords: Aluminium matrix composites (AMC), Fatigue, nanoparticles, Silicon carbide (SiC), Stir casting technique (SCT), Titanium dioxide (TiO_2).

1. Introduction

Many improvements have been made to manufacturing metal matrix composites, including the mechanical alloying technique, in preparing an aluminium-based composite material reinforced with cement (Fe_3C). For powders, the time and temperature of hot pressing and the examination results showed excellent compatibility between the substrate and the reinforcing material represented by the particles [1-4]. The researcher [5-8] also used powder metallurgy technology when preparing a composite material from tool steel as a substrate reinforced with particles to control the uniform distribution of particles with high-volume fractions within the substrate.

Awad et al. [9] used the filtering squeeze technique to reach the best penetration of the mineral liquid in the interspaces of the group of short fibres and to increase the wetting of the fibres of the base material, which gave the composite material better properties. Recent research has also tended to study the effect of casting elements and the reinforcing materials added to them, and there are conflicting results about the effect of the size and shape of the added reinforcement materials on the solidification mechanism by dispersing these particles. To the need for more influence of these materials in the solidification mechanism of these alloys. They noticed that the base metal alloy penetrated between the tungsten carbide particles and interacted with the particles during the manufacturing process. The interface's properties depend on the substrate's physical and chemical properties and the hardness of the reinforcing particles [10, 11].

About the microstructure, Maindal [12] studied the effect of the weight fraction of the reinforcing material (TiB) on the extent of the needle distribution of the alloying element (Si) inside the base material (Al-7Si). They noticed that an increase in the weight fraction of the reinforcing particles leads to a decrease in the growth of the needle size of the silicon, and they attributed this to the fact that the reinforcing material works to reduce the needle growth of the silicon [12,13].

In the field of nanocomposite materials, [14, 15] produced a nanocomposite Cu-FeC by preparing a composite material by the mechanical casting of the elements, Fe Cu graphite, and subsequent heat treatment. The studies included the possibility of separating the components of the composite material. Yu et al. [16] and Hayfaa and Abbas [17] separated the aluminium substrate from the reinforcing material SiC from the scrap materials (Scrap) for the composite Al - SiC by adding a salt auxiliary melting agent to the molten alloy. Concerning the properties of fatigue for aluminium and its alloys and composite materials, it has been observed that the behaviour of fatigue depends on the methods of manufacturing the materials and on other factors, including the surface condition, the type of substrate, the reinforcing materials, the volume fraction, and the particle size of the reinforcement particles and how they are distributed within the substrate, as well as the heat treatment suffix.

In a study on the growth of fatigue cracks along the grain boundaries of Al–Mg–Si alloy, the study showed that the rate of fatigue crack growth decreases with an increase in the aging time as the magnesium precipitates and sequesters at the grain boundaries and the hydrogen concentration increases at the top of the crack [18, 19]. The fatigue crack growth rate of Al 2524-T3 alloy was also studied (before and after long heat treatment at 130 °C and for 100 and 1000 hours). The effect of the trend disappears after a long heat treatment at 130 °C [20]. In a study on the effect of surface treatment on the fatigue properties of Al 2024-T3 alloy, it was noted that the fatigue behaviour is similar for both alloys whether and not heat treated [21, 22].

Several studies are concerned with the fatigue properties of the composite material based on aluminum alloys, which depend on the volume fraction of the reinforcement particles, most of which are supported by (SiC) [23, 24]. In a recent study on the effect of the volume fraction of (SiC) particles on the failure cycles of (2124\Al - Si - Cu) alloy prepared by powder metallurgy technique and AS7G \ Al-Si - Mg alloy prepared by casting technology, a decrease in fatigue resistance was observed. of the matrix composite AS7G compared to the fatigue strength of the matrix 2124**.** Through the microscopic examination of the samples with a scanning electron microscope (SEM), it was noted that the beginnings of fatigue cracks of the substrate AS7G occur at the interface (\SiC matrix), and it was noted that there are large numbers of interfaces lacking bonding (De-bonding). Between the matrix AS7G and the reinforcing particles SiC, this was attributed to the decrease in the fatigue resistance of the AS7G matrix composite [25, 26].

The current research aims to study the effect of adding titanium oxide TiO_2 nanoparticles on the one hand and silicon carbide (SiC) nanoparticles on the other hand with different weight ratios of 0, 3, 6 and 9 wt.% with fine grain sizes to the base alloy Al-2Cu-2Mg with Wide applications and study of the weight fracture effect of both titanium oxide TiO_2 and silicon carbide SiC nanoparticles in the hardness and fatigue behaviour of the composite material prepared by mixing casting technique. The study included the effect of double heat treatment on the hardness values of both the base alloy and the composite material.

2. Experimental Work

The base alloy consisting of Al - 2Cu - 2Mg was prepared by melting pieces of aluminium with purity 99.8% of known weight in a crucible of graphite to a temperature of 800 °C, then adding a chip of pure copper with a weight ratio of 4 % from aluminium. After that, a chip of pure magnesium with a weight ratio of 1% was added to the melt of the alloy with continuous stirring, and then the molten was poured into cylindrical moulds made of solid iron and preheated at a temperature of 300 ° C. Table 1 displays the mechanical and physical properties of Nano SiC and TiO_2 [27] and Table 2 chemical analysis of the base alloy.

Table 1. Experimental values of mechanical and physical properties of nano SiC and TiO_2.

Nano	Compressive strength (MPa)	VHN (GPa)	E (GPa)	Density gm/cm^3	Melting point (^{o}C)	Particle size (nm)
SiC	3009	29	415	3.1	2830	20-40
TiO_2	3118	38	431	4.23	1843	20-40

Table 2. Chemical analysis of the base alloy [27].

Base Alloy	Wt. % Al	Wt. % Cu	Wt. % Mg
Al - 2Cu - 2Mg	96	2	2

As for the Metal Matrix, they were prepared in two groups, depending on the stiffeners:

- Group A: The first group (G1): composite materials consisting of (Al-2Cu-2Mg) fortified with TiO2 minerals with a purity of 99.8 % and with different weight ratios (0,3,6,9 wt.%).

- Group B: The second group (G2): composite materials consisting of (Al-2Cu-2Mg) reinforced with SiC nanoparticles with purity of 99.8% and with different weight ratios (0, 3, 6, and 9 wt.%) [28].

Samples were cut 2 cm in length as models for testing hardness, microscopy, and X-ray diffraction, and the rest of the samples were used in preparing samples for testing both fatigue and tensile strength. The heat treatment of the prepared samples was carried out for each of the base alloy and the compound materials produced for thermal homogeneity and the elimination of some plumbing defects such as isolation and to ensure a homogeneous distribution of phases in the cast. The solution treatment was carried out at a temperature of 500 °C for 4 hours, then quenching with cold water, followed by an industrial aging process for samples intended for testing the hardness at a temperature of 160 °C for a period of two hours, and then industrial aging at a temperature of 180 °C, with different periods between 0.5-5 hours. The maximum tensile strength of the base alloy was tested and was equal to 270 MPa. An X-ray diffraction test was performed to determine the phases of the base alloy and the overlaying materials after thermal solution treatment and aging. The twelve types of samples were used in the tensile test. Three samples were taken for each case, and the average of the three readings was taken. A programmed CNC turning machine is used to machine all of the samples. Figure 1 shows the tensile test specimen on which testing is performed by ASTM (E8/8M-09) 2010 [29-31].

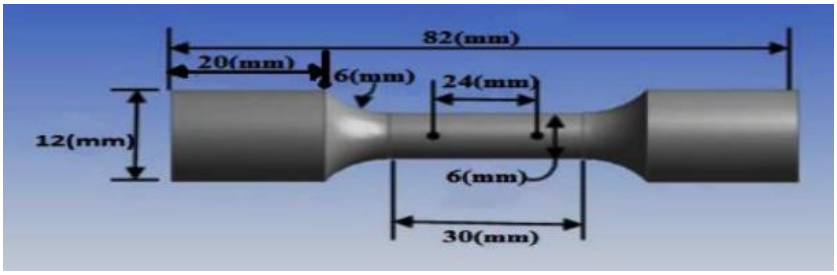

Fig. 1. Tensile test specimen [28].

The Twelve samples were manufactured with bars and different lengths at a rate of three samples for each case. Test samples were manufactured by CNC programmed lathe at the Institute of Technology - Baghdad to obtain high accuracy in the sample, avoid any errors in the dimensions, the process of softening surfaces, and obtain good surface roughness to reduce the remaining stresses. Figure 2 shows the dimensions of the sample used in rotational bending fatigue tests [32].

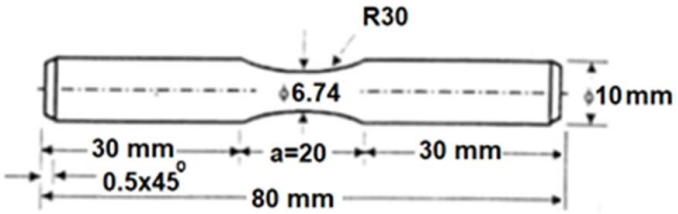

Fig. 2. Fatigue specimens (ASTM) according to (DIN 50100) standard specification [29].

3. Results and Discussion

3.1. X-Ray diffraction testy results

The X-ray diffraction patterns at room temperature for the base alloy and the alloys reinforced with SiC nanoparticles on one side and TiO2 nanoparticles on the other, after the solution and aging treatment, are shown in Figs. 3(a), (b) and (c), respectively. The X-ray diffraction patterns at room temperature for the base alloy and the alloys reinforced with SiC nanoparticles on one side and TiO2 nanoparticles on the other, after the solution and aging treatment, are shown in Figs. 3(a), (b) and (c), respectively.

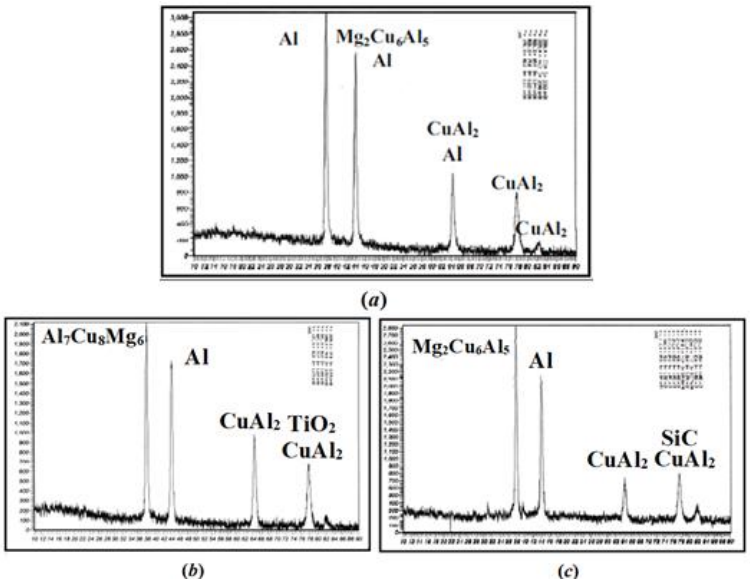

Fig. 3. X-ray diffraction patterns after solution treatment, forming, and aging: (a) the base alloy, (b) the composite material reinforced with TiO_2. nanoparticles, and (*c*) the composite material reinforced with SiC nanoparticles.

The phases formed in these samples are shown in Tables 3 to 5. Superimposed, as well as the appearance of minerals of both TiO_2 and SiC and represented by the second phase $CuAl_2$, which is shown by the three tables and according to the angles of their appearance. Table 4 also shows the emergence of the SiC phase at an angle of 79.8° and the TiO2 phase in Table 5 at an angle of 80.1°.

Table 3. Results of X-ray diffraction examination of the Al - 2Cu - 2Mg base alloy after casting, solution treatment, forming, and aging at a time of 2 hours.

2θ	dm (A°)	ds (A°)	Phase	I /Io
39.1	2.4	2.4	Al	100
45.5	2.1	2.1	Al	48
45.5	2.1	2.1	$Mg_2Cu_6Al_5$	41
66.3	1.4	1.7	Al	21
66.3	1.4	1.5	$CuAl_2$	8
80.1	1.3	1.6	$CuAl_2$	15
84.6	1.2	1.2	$CuAl_2$	4

Table 4. Results of X-ray diffraction examination of the composite base alloy (Al - 2Cu - 2Mg) reinforced with SiC minutes after casting, solution treatment, forming, and aging at a time of two hours.

2θ	dm (A°)	ds (A°)	Phase	I /Io
38.8	2.41	2.43	$Al_7Cu_8Mg_6$	100
45.2	2.11	2.08	Al	48
66.1	1.48	1.45	$CuAl_2$	41
79.8	1.25	2.27	$CuAl_2$	21
79.8	1.25	1.29	SiC	8
84.3	1.20	1.19	$CuAl_2$	15

Table 5. Results of X-ray diffraction examination of the composite base alloy reinforced with TiO_2 nanoparticles after casting, solution treatment, forming, and aging at a time of two hours.

2θ	dm (Ao)	ds (Ao)	Phase	I /IO
38.8	2.41	2.43	Al7Cu8Mg6	100
45.3	2.11	2.08	Al	48
66.3	1.48	1.45	CuAl2	41
80.1	1.25	2.27	CuAl2	21
80.1	1.25	1.24	TiO2	8
84.4	1.20	1.19	CuAl2	15

3.2. Results of the hardness test

Figure 4 shows the effect of the aging time on the hardness values of the base alloy (Al-2Cu-2Mg) after performing the solution treatment at 500 °C and aging at a temperature of 160 °C for two hours and then aging at a temperature of 180 °C, during periods ranging from 0.5 - 5 hours. It is noticed that the hardness of the base alloy after casting and the solution treatment increases with the increase of the aging time to reach its highest value at an aging time of 4 hours. The alloy and its resistance gradually increase. When the aging period is increased to more than 4 hours, the hardness values decrease, and this is due to the accumulation of sediment nanoparticles and the formation of larger nanoparticles, as well as the loss of the emotions of correspondence between the ground and the deposited facts. In addition, the heat treatment creates intermediate phases resulting from the diffusion processes of the alloying elements, copper, and magnesium. This is what is certified by the results of the X-ray diffraction examination in Table 4 as it is observed that the phase ($Mg_2Cu_6Al_5$) appears, which delays the phase deposition process ($CuAl_2$) and, thus, a decrease in the rate of formation of obstacles to the movement of dislocations, which leads to a decrease in the hardness values.

As for after the formation process and solution treatment, it is noticed that the base alloy's hardness has increased compared to before forming and a decrease in the time required to reach the maximum hardness values. This is because the cold-forming process increases the number of crystalline defects, which increases the resistance values. Tensile strength, low plasticity, and cold forming increase the speed of aging due to the formation of many voids, which contribute to the rapid spread of sediment phases, that is, an increase in the speed of transformation processes in the structural structure of the alloy. Figure 5 shows the effect of the weight ratio of SiC and TiO_2 minutes added to the base alloy on the hardness values

of the prepared compound materials represented by two groups (G1 and G2) after performing the solution treatment at a temperature of 500 °C. The hardness values of the base alloy increase with the increase in the addition ratios of TiO_2 or SiC nanoparticles to them. Minutes larger than one-micron act as obstacles to the deformation of the base alloy due to its high hardness, and those with a volume of fewer than 0.2 microns dispersed within the base alloy structure will impede the dislocations formed in the substrate.

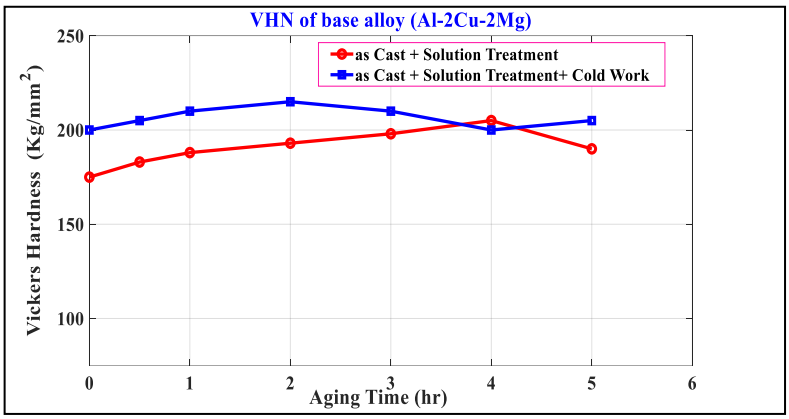

Fig. 4. The effect of aging on the hardness values of the base alloy.

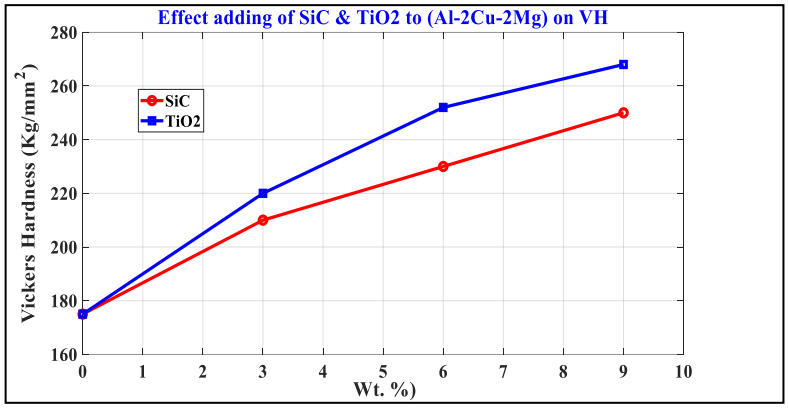

Fig. 5. Effect of minute weight ratio effect of SiC and TiO_2 added to the base alloy in hardness values.

Also, the rate of increase in the hardness values of the base alloy increases with the increase in the rates of addition of both TiO_2 and SiC nanoparticles, and this can be explained by the fact that when these minutes penetrate the base structure with different weights ratios and sizes, some factors, this will change some factors, including the minute spacing. It is noticed from the figure that the rate of increase in hardness values is symmetric in both groups, although the hardness values of group (B) are slightly higher than they are in group (A). The maximum tensile strength (UTS) of TiO_2 300-600 MPa SiC is 200-500 MPa, respectively, while the Young Modulus of TiO_2 is 325-430 GPa and SiC is 250-410 GPa, respectively.

Figure 6 shows that adding the strengthening minutes does not affect the aging stages. All alloys' hardness values increase with increasing aging time to reach their maximum values at a 4-hour aging period and then to increase the hardness values.

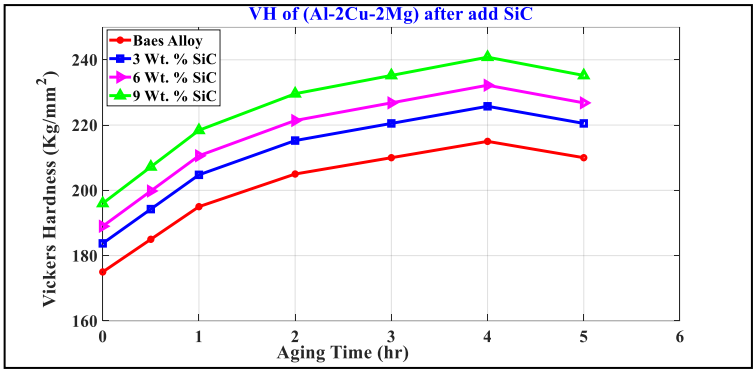

(a)

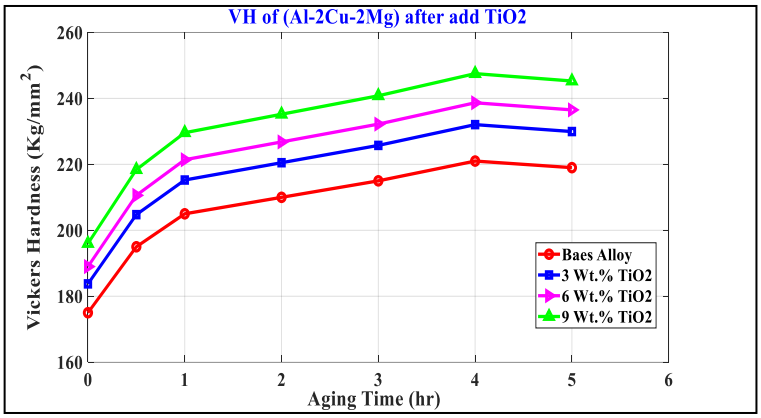

(b)

Fig. 6. The effect of the duration of artificial aging on the hardness values of the base alloy reinforced with (a) SiC and (b) TiO_2.

3.3. Result of fatigue test

Figure 7 shows the results of the fatigue test of the base alloy. It is noted that at high-stress amplitude, the number of failure cycles is small due to the Elastic-Plastic-Fracture Mechanism (EPFM), which occurs on the surface of the metal, leading to crack growth that leads to failure. However, when the stress capacity is low, the number of cycles leading to failure is high due to the elastic failure known in the Linear Elastic Fracture Mechanism (LEFM).

From Figs. 8 and 9 of the base alloys and the alloys reinforced with TiO_2 nanoparticles on the one hand and SiC nanoparticles on the other hand, respectively, it is noted that strengthening the base alloy with TiO_2 or SiC nanoparticles led to an increase in the resistance of all than it is in the base alloy and that the rate of increase increases with the increase in weight ratios.

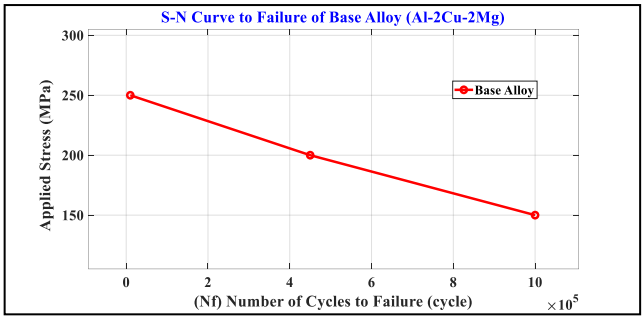

Fig. 7. The relationship between stress amplitude and N_f of failure cycles of the base alloy.

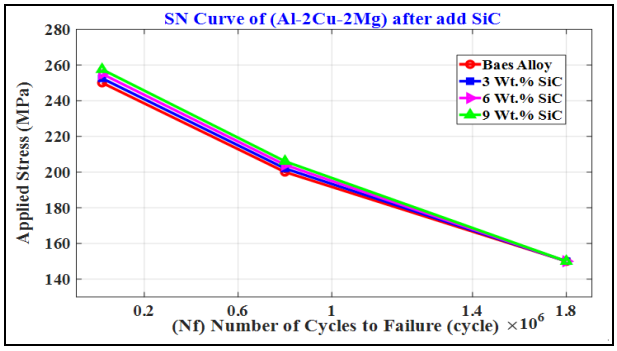

Fig. 8. The relationship between the stress amplitude and the Nf for both the alloy and the alloy reinforced with TiO_2 nanoparticles, with weight ratios 0%, 3%, 6%, 9 %.

For the added particles, this increase in the fatigue resistance values is due to the nature of these hard particles distributed in the base alloy with different molecular sizes, which increases the strength of the alloy through the dispersion hardening mechanism, which leads to an increase in the number of failure cycles for the alloys reinforced with these facts.

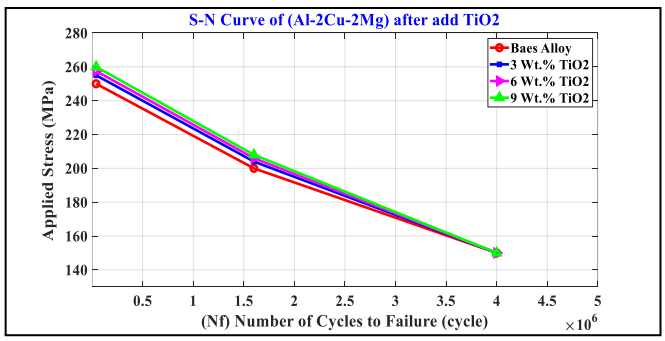

Fig. 9. The relationship between stress amplitude and Nf for the base alloy and the SiC powder reinforced alloy with 0%, 3%, 6%, and 9 wt.%.

To clarify the study of the effect of the added weight percentages of the reinforcing particles on the failure cycles of the prepared alloys, a graphical relationship was established between the number of failure cycles and the added weight percentages of the reinforcing particles under the constant stress of 150, 250, 350 MPa, represented in Figs. 10-12, respectively.

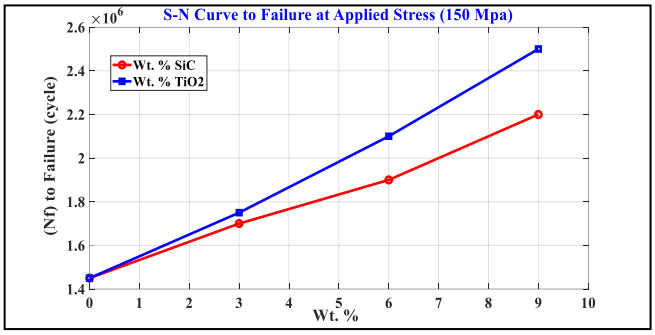

Fig. 10. The relationship between the number of failure cycles and the percentage of strengthening minutes added with a 150 MPa loading stress constant.

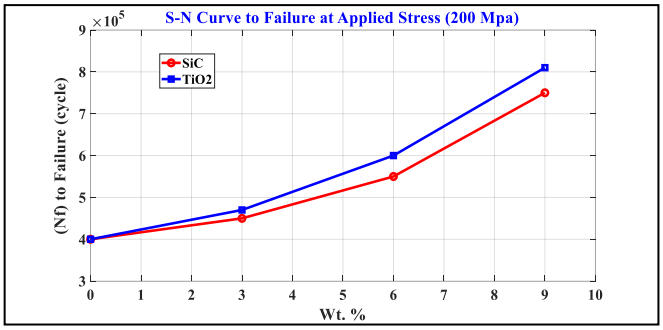

Fig. 11. The relationship between the number of failure cycles and the percentage of strengthening minutes added with a 250 MPa loading stress constant.

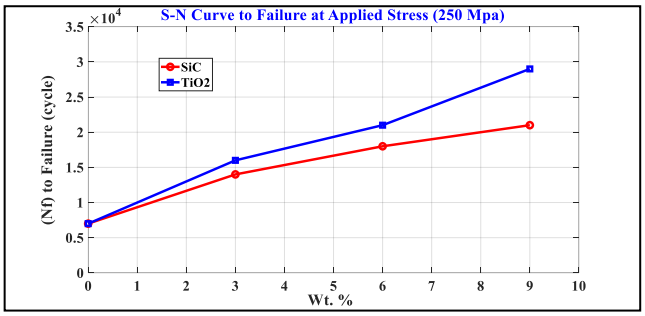

Fig. 12. The relationship between the number of failure cycles and the percentage of strengthening minutes added with a 350 MPa loading stress constant.

It has been realized that the rate of increase in the values of fatigue strength is symmetric in both groups (A and B) except for a slight difference in the number of failure cycles (N_f) for the group (B) supported with TiO_2 nanoparticles compared with a group (A) supported with SiC minutes. This is due to the higher mechanical properties of TiO_2 nanoparticles compared to SiC nanoparticles.

The increase in hardness and the number of failure cycles when checking fatigue can be attributed to the presence of TiO_2 or SiC nanoparticles in the base alloy with different weight ratios that change the distance between minutes in addition to the change in the free path rate, which is inversely proportional to the fracture. The volume of the added substance (V_S) is according to the following relationship:

$$V_S = \frac{2d}{3V_P}(1 - V_P) \quad (1)$$

where d: Substance volume (microns) and V_p: volumetric fraction of substance added.

The presence of such minutes will impede the movement of dislocation, and the rate of disability will be greater when the weight ratios of the added minutes are increased. For the dislocation to pass through the dispersed nanoparticles in the base alloy phase, the exerted stress must be sufficient for the dislocation bend. This stress (T) is inversely proportional to the distance between minutes (D) and according to the following relationship:

$$T_i = \frac{G_m * b}{D_p} \quad (2)$$

where: Gm: shear modulus of the base alloy and b: Berger vector.

It is evident from this relationship that upon the homogeneous dispersion of the strengthening minutes, the distance between the minutes (Dp) will decrease with the increase of the percentage of added minutes. Therefore, it will require greater stress to pass the dislocation during these minutes and thus increase the values of both hardness and fatigue resistance.

3.4. Results of the microstructure test

The microstructure of the base alloy Al- Cu - Mg before and after the solution treatment and aging is a solid solution consisting of copper in aluminum. The enlargement of the nanoparticles and the presence of plumbing defects such as gaps and isolation were observed as fine and somewhat homogeneous granules. Figures 13 and 14 show the microstructure of the composite material reinforced with SiC and TiO_2 minerals, respectively, before and after the solution treatment.

This is confirmed by the results of X-ray diffraction by the emergence of the phases represented by SiC, shown in Fig. 14(b) and Table 4 at the angles 79.8, as well as the phases represented by TiO_2 and shown in Fig. 14(c) shown in Table 4.

When the angle 80.1, as well as the precipitated phase and its homogeneous distribution, which is confirmed by the results of the X-ray examination in Fig. 14 and shown in Table 4, related to the X-ray diffraction with the appearance of the second phase $CuAl_2$ in the base alloy and the material Overlay. It is also noted that the strengthening minutes overlapped between these phases.

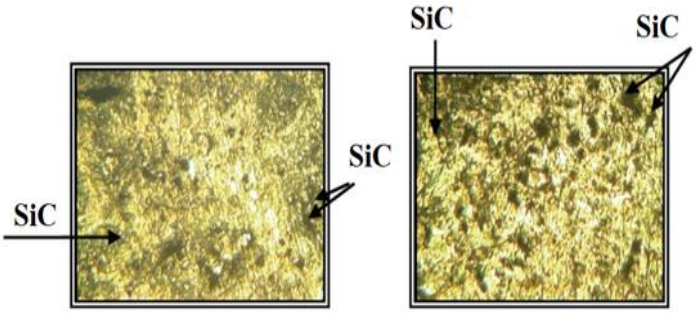

(a) A Composite material plus (9%) (SiC), (b) A Composite material plus (9%) (SiC)

before the treatment after the treatment

Fig. 13. Microstructure of the composite material (a and b) reinforced with SiC nanoparticles before and after the solution treatment. (300x).

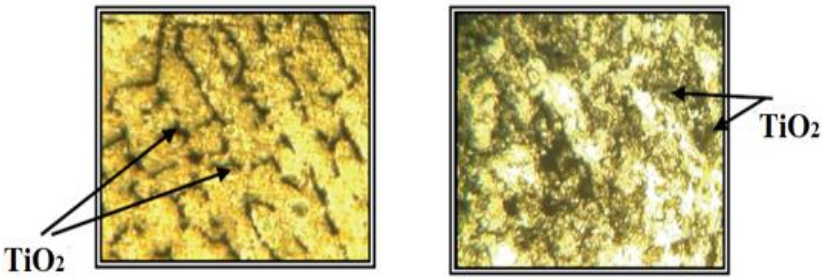

(a) A Composite material plus (9%) (TiO2), (b) A Composite material plus (9%) (TiO2)

before the treatment after the treatment

Fig. 14. Microstructure of the composite material (a) and (b) reinforced with TiO_2 nanoparticles before and after the solution treatment. (300x).

4. Conclusions

The aging time needed for the base alloy and the resultant composite material to reach their maximum hardness values was shortened by the forming procedure and heat treatment. Hardness values increases with the addition of SiC and TiO_2 nanoparticles. The proportion of this rise grew as the percentage of additional minutes increased. The highest hardness values of all the produced alloys supplemented with TiO_2 or SiC nanoparticles were obtained after four hours of age. The resulting composite exhibits higher fatigue strength and hardness than the base alloy, and these values rise as the weight ratios and base alloy's additional stiffness increase. The composite material reinforced with TiO_2 nanoparticles exhibits higher fatigue strength and hardness values in comparison to the composite material reinforced with SiC nanoparticles. They still have better mechanical qualities than the base alloy in both situations. The findings of the X-ray diffraction test revealed the emergence of SiC and TiO_2 nanoparticles, as well as second phase $CuAl_2$ minutes in the base alloy and the overlaid material.

Acknowledgment

This research work is supported by the University of Baghdad, College of Engineering, Mechanical Engineering Department with the University of Technology and Al Safwa University College - Iraq.

Nomenclatures

B	Berger vector.
D	Minute volume (microns)
D_p	The distance between the minutes
G_m	Shear modulus of the base alloy
T	Stress
V_S	Volumetric fraction of substance added

References

1. Eugene, E.F.; Larisa, N.D.; and Justyna, P.M. (2021). On Investigating the microstructural, mechanical, and tribological properties of hybrid FeGr1/SiC/Gr. *Metal Matrix Composites Materials*, 14(174)
2. Jamaluddin, H.; Kini, A.; and Murthy, A. (2018). Mechanical characterization of precipitation hardened Al7075-Grey cast iron powder reinforced metal matrix composites. *MATEC Web of Conferences*, 144 - 02007.
3. Assi. A.D. (2020). Influence of Al2O3 nanoparticles addition to AA6082-T6 on mechanical properties by stir casting technique. In *Proceedings of 3rd International Conference on Sustainable Engineering Techniques* (ICSET 2020), *IOP Conference Series: Materials Science and Engineering*, 881 - 012081.
4. Suswagata, P.; Goutam, S.; and Prasanta, S. (2021). Abrasive wear behaviour of Al-Tib_2 and Al-Tib_2-Nano-Graphite metal matrix composites. In *Proceedings of the Institution of Mechanical Engineers, Part L: Journal of Materials: Design and Applications*, 235(1).
5. Andre M.; Inam, U.A.; Reza, M.; Yan, D.; and Dermot, B. (2021). Advanced production routes for metal matrix composites. *Engineering Reports*, 3, e12330.
6. Daisy. N.; Siebeck, S.; Podlesak, H.; Wagner, S.; Hockauf, M.; and Wielage, B. (2016): Powder metallurgy of particle-reinforced aluminium matrix composites (AMC) by means of high-energy ball milling**.** In: Fathi, M., Holland, A., Ansari, F., Weber, C. (eds) *Integrated Systems, Design and Technology 2010*. Springer, Berlin, Heidelberg.
7. Assi, M.D.; Hassan, A.A.; and Salman, H.O. (2020). Effect of adding SIC and TiO_2 nanoparticles to AA6061 by stir casting technique on the mechanical properties of composites. *Journal of Mechanical Engineering Research and Developments*, 43(6), 167-183.
8. Kargul, M.; Borowiecka, J.J.; and Konieczny, M. (2019). The effect of reinforcement particle size on the properties of Cu-Al2O3 composites. In *Proceedings of the 5th International Conference Recent Trends in Structural Materials*, IOP Series: *Materials Science and Engineering*, 461, 012035.

9. Awad, M.; Hassan, N.M.; and Kannan, S. **(**2021**).** mechanical properties of melt infiltration and powder metallurgy fabricated aluminium metal matrix composite. *Proceedings of the Institution of Mechanical Engineers, Part B: Journal of Engineering Manufacture*, 235(13), 2093-2107.
10. Fereiduni, E.; Ghasemi, A.; and Elbestawi, M. (2019). Selective laser melting of hybrid ex-situ/in-situ reinforced titanium matrix composites: laser/powder interaction, reinforcement formation mechanism, and non-equilibrium microstructural, evolutions. *Materials & Design* 184 - 108185.
11. Safaa, M.H.; Qasim M.A.; Assi; A.D.; and Mustafa, K.I. (2020): The role of ZnO Nano-fluids on heat treatments of medium carbon steel. In *Proceedings of the 3rd International Conference on Sustainable Engineering Techniques* (ICSET 2020), *IOP Conf. Series: Materials Science and Engineering*, 881, 012095.
12. Maindal, A.; Chakraborty, M.; and Murty, B.S.; (2004). Microstructural evolution of Al–Si based composites reinforced with in – situ TiB2 particles. *International Symposium of research students on Material Science and Engineering*, ISRS- 2004, 20-22.
13. Dariusz, B.; Aneta, B.: Paweł, P.; Jakub, H.; and Adam, P. (2020). Characterization of W–Cr metal matrix composite coatings reinforced with WC particles produced on low-carbon steel using laser processing of precoat. *Materials*, 13, 5272.
14. Carvalho, P.A.; Fonseca, I.F.; Marques, M.T.; Correia, J.B.; Almeida, A.; and Vilar, R. (2005). Characterization of copper-cementite nano composite produced by mechanical alloying. *Acta Materialia*, 53, 967-976.
15. Ravi, K.R.; Pillai, R.M.; Pai, B.C.; and Chakraborty, M.; (2007). Separation of matrix alloy and reinforcement from aluminium metal matrix composites scrap by salt flux addition. *Bulletin of Materials Science*, 30, 393-398.
16. Yu, W.; Yunlai, D.; Jiqiang, C.; Qingsong, D.; and Xiaobin, G. (2020). Effects of grain structure-related precipitation on corrosion behaviour and corrosion fatigue property of Al–Mg–Si alloy. *Journal of Materials Research and Technology*, 9(3), 5391-5402.
17. Hayfaa, D.H.; and Abbas, A.A. (2019). Flexural performance of laced reinforced concrete beams under static and fatigue loads. *Journal of Engineering*, 25(10).
18. Chen, Y.; Xiong, C.; Liu, W.; Pan, S.; Song, Y.; Liu, Y.; and Zhu, B. (2021). Texture evolution and control of 2524 aluminium alloy and its effect on fatigue crack propagation behaviour. *Applied Sciences*, 11, 5550.
19. Abdullah, A.A.; and Munther, A.M. (2019). An experimental and numerical investigation of heat transfer effect on cyclic fatigue of gas turbine blade. *Journal of Engineering*, 25(7).
20. Mariana, P.M.; and Shoshan T.A.; (2021). Theodor Hack, Malte Burchardt and Herman Terryn, a review on anodizing of aerospace aluminium alloys for corrosion protection**.** *Coatings*, 10 -1106.
21. Abdulridah, M. N.; Assi, A.D.; and Al-Alkawi, H.J. (2020). Influence of cryogenic temperature (CT) on tensile properties and fatigue behaviour of 2024-Al2O3 nanocomposites. *ICEMEA-2020, IOP Conference Series: Materials Science and Engineering*, 765 - 012052.

22. Ali, N.A.; Ali, H.A.; and Ahmed, R.A. (2019). mechanical properties enhancement of conventional glass ionomer cement by adding zirconium oxide micro and nanoparticles. *Journal of Engineering*, 25, (2).
23. Maleque, M.A.; Adebisi, AA.; and Izzati, N. (2021). Analysis of fracture mechanism for Al-Mg/SiCp composite materials, *IOP Conference Series: Materials Science and Engineering* 184 – 012031.
24. Zhiyu, Y.; Fan, J.; Liu, Y.; Nie, J.; Yang, Z.; and Kang, Y. (2021). Strengthening and weakening effects of particles on strength and ductility of SiC particle reinforced Al-Cu-Mg alloys matrix composites. *Materials*, 14, 1219.
25. Hansen Z., Zhifeng Z.; and Yuelong B. (2021). Numerical simulation and experimental study on compound casting of layered aluminium matrix composite brake drum. *Materials*, 14, 1412.
26. Bayraktor, E.; Masounave, J.; Caplain, R.; and Bathias C.; (2008). Manufacturing and damage mechanisms in metal matrix composites. *Journal of Achievements in Materials and Manufacturing Engineering*, 31(2), 294-300.
27. MatWeb.com, Material Property Data. Available at: https://www.matweb.com/help/PropertyDataAvailability.aspx (retrieved on April 2023).
28. ASTM E8/E8M - 09 **(**2010**)**. *Standard test methods for tension testing of metallic materials*. ASTM International, 03.01.

    https://www.astm.org/Standards/E8
29. DIN 50100 - (2016). *DIN 50100 Load controlled fatigue testing - execution and evaluation of cyclic tests at constant load amplitudes on metallic specimens and components*. EUROLAB, Mechanical Tests.
30. Porter, D.A.; Easterling, K.E.; and Sherif, M.Y. (2021). *Phase transformations in metals and alloys*. 4th Edition, Taylor & Francis Group, CRC press, Boca Raton.
31. Michael, F. A.; David, R.; and Jones, H.; (2019). *Engineering Materials*, Fifth Edition, Published Elsevier Ltd. Press, Hungary.
32. ASTM (2012). *Standard specification for aluminium and aluminium-alloy shaft and rode*. ASTM, USA.